Spatial Variation of Stiffness and Edge Beam Participation in RC Box Culverts

Syed Mujtaba Haider[1]

[1]Department of Civil and Environmental Engineering, Auburn University

ABSTRACT

Reinforced concrete (RC) box culverts exhibit a non-uniform structural response under two-patch localized loading due to plate action and boundary elements at the opening that are not accounted for in conventional 2-D models for design and analysis purposes. This paper addresses the spatial variation in the stiffness of RC box culverts with and without edge beams, using linear-elastic finite-element analysis. Stiffness was derived from the load-deflection responses at various locations along the culvert length. The results show that the stiffness depends on the load location, indicating that the culvert system does not behave as a uniform structural element. The presence of the edge beam leads to local stiffness amplification near the opening, which gradually diminishes towards midspan. The reaction distributions also indicate that the edge beam acts primarily as a boundary stiffener and that the global load-transfer mechanism remains unchanged. The contribution of the edge beam was isolated using a relative stiffness parameter that exhibits a consistent exponential-decay trend across different spans. Based on these observations, a span-sensitive formulation was developed to describe this behavior as a function of distance, and it showed good agreement with finite-element results (R2 = 0.979). The proposed framework offers a physically interpretable representation of edge-beam stiffness participation in an indeterminate structure and adds to a better understanding of the load distribution behavior in the culvert with and without edge beams.

1. INTRODUCTION

1.1 Plate Behavior in RC Box Culverts

Reinforced concrete (RC) box culverts are widely used as short-span bridge systems. The structural response of these structures to localized loading is dominated by plate action and boundary interactions rather than beam behavior. The load transfer mechanism in box culverts is by two-way slab action with the vertical sidewalls providing the rotational restraint along the edges of the slab. Thus the system behaves as a plate with semi-rigid boundaries, the stiffness and load distribution being dependent on geometry and boundary conditions. Reinforced-concrete slab bridge systems are characterized by similar plate-based load distribution mechanisms where the structural response is dominated by slab action, and influenced by boundary conditions and edge elements (Mabsout et al. 2004)). The previous studies on box culverts have mainly concerned their behavior under different loading conditions such as live load effects, soil cover and structural response during their service life (Abdel-Karim et al. 1993; Orton et al. 2015; Liu et al. 2018; Ulger et al. 2020; Moradi et al. 2015; Woo et al. 2010; Bentz et al. 2007). These investigations have primarily focused on the global response, including load distribution due to soil, cracking behavior, flexural and shear capacity, and overall structural performance. However, the mechanics underlying spatial variation in stiffness along the culvert, especially due to the presence of an edge beam as a boundary element, have not yet been examined in detail. Contrary to the assumed design and analysis model assumption, the structural response is not uniform along the length of the culvert when loaded in a concentrated manner. The longitudinal evolution from boundary-dominated behavior to global plate behavior is central to this present study.

1.2 Edge Beams and Boundary Stiffening

Edge beams are often introduced at the culvert opening. These elements offer additional rotational confinement along the slab edge. Their application is well known in practice, but the effect of the edge beams on the distribution of spatial stiffness and load transfer has not yet been fully examined and quantified. Mechanically, the presence of an edge beam alters the boundary conditions of a culvert's slab, thereby increasing the stiffness at the opening. Boundary rotational stiffness has been found to be a key factor governing the deformation and stiffness responses of plate systems ((Hu and Adams 2017). The interaction of plate stiffness and boundary rigidity also affects the distributions of moments, reactions, and deflections in slab systems ((Fuchs 1954). However, in plate systems such boundary stiffening is not limited to the immediate vicinity of the opening. Instead, the effect propagates along the length of the culvert and slowly decays due to stiffness compatibility and load redistribution. However, the current studies do not provide a quantitative description of the spatial variation in edge-beam-induced stiffness or the degree of influence along the culvert length.

2. NUMERICAL MODELING AND STIFFNESS EXTRACTION FRAMEWORK

2.1 Geometry and Boundary Conditions

Three-dimensional finite element models of single-cell RC box culverts were developed to capture the global plate response and the longitudinal load sharing. The culvert system consists of a top slab (0.254m), monolithically connected to vertical sidewalls (0.2m), and a bottom slab(0.254m), forming a closed box structure. The opening edge was explicitly modeled as the edge beam (width by depth = 0.254 m × 0.584 m), where boundary effects are expected to be most significant. Multiple span lengths were considered to study the effect of structural scale on the distribution of stiffness and the spatial decay behavior. For each span length, the culvert length was selected such that the transition from the boundary-dominated response near the opening to the stabilized plate action in the middle span is captured. The length of the culvert was chosen to be sufficiently long to include the transition from the boundary-dominated response near the opening to the stabilized plate action toward midspan for each span.

Boundary conditions were defined to represent realistic support behavior while maintaining analytical clarity. The base of the culvert was restrained to simulate vertical support conditions, and symmetry conditions were applied at one end to reduce computational cost without influencing longitudinal response. This modeling framework enables direct evaluation of how localized boundaries stiffening at the opening propagates along the slab and influences global structural behavior.

2.2 Material Modeling and Service-Level Assumption

Concrete was modeled as a linear elastic, homogeneous material to isolate stiffness-controlled behavior in the pre-cracking regime. The objective of this study is not to capture nonlinear damage mechanisms, but to quantify the relative stiffness participation associated with the presence of edge beams.

The use of linear elasticity is justified for three primary reasons. First, the study focuses on stiffness comparison rather than strength or ultimate capacity. Second, incorporating nonlinear cracking would introduce stiffness degradation that could obscure the boundary-stiffening effect of the edge beam. Third, service-level structural behavior, including load distribution and stiffness response, is largely governed by elastic properties prior to significant cracking.

By restricting the analysis to the linear elastic range, the extracted stiffness values represent the structural response governed by geometry and boundary conditions. This allows for consistent comparison of stiffness amplification and spatial decay across different configurations.

2.3 Loading Protocol

Realistic tire contact areas (0.254 m × 0.508 m) were simulated by applying the wheel loads as surface pressure patches to the top slab. For each culvert configuration of span=3.04m, 4.26m and 5.48m as shown in Figure 1, Figure 2 and Figure 3, respectively, load patches were located at five discrete longitudinal distances from the opening to capture the spatial variation in culvert slab stiffness. A load control approach was used to ensure consistency across all configurations and to enable direct comparison of load-deflection behavior. The use of pressure patches enables a realistic representation of vehicular loading and the evaluation of load transfer through the plate system. For each load position, the representative stiffness was extracted from the load-deflection response. Furthermore, reaction forces along the culvert walls were measured to study load distribution. This method guarantees that stiffness comparisons are made under the same loading conditions and also allows a separate evaluation of load-flow behavior through reaction distributions.

2.4 Stiffness Extraction and Reaction Evaluation

The representative stiffness was defined as the slope of the load-deflection response in the linear elastic region. The deflection was recorded at the center of the applied load patch, not at the point of maximum deflection. This choice guarantees that all configurations are identical. In plate systems, the maximum deflection position can vary with the boundary stiffness conditions. This would thus confound two effects in the evaluation of stiffness at a moving peak location: (i) changes in boundary stiffness and (ii) spatial redistribution of deformation.

Reaction forces along the sidewalls were extracted and normalized over the culvert length; the distributions of these reactions are an independent measure of load-transfer mechanisms. The global load path is preserved if normalized reaction profiles are similar for the different configurations. Magnitude differences indicate local stiffness modifications. The stiffness extraction and reaction evaluation procedures combined provide complementary insight into (i) the spatial variability of the effective stiffness, (ii) the longitudinal decay of boundary-stiffening effects, and (iii) the preservation of the global plate action.

3. MECHANICS OF BOUNDARY STIFFENING AND LONGITUDINAL DECAY

3.1 Boundary Stiffening and Rotational Restraint

In plate systems, structural response is governed by compatibility between bending curvature and boundary conditions. If a slab is monolithically connected to the supporting edge beam, then the boundary is provided with rotational restraint. The magnitude of the rotational restraint directly affects the local curvature demand. The addition of an edge beam increases the flexural rigidity at the opening boundary. This modification changes the effective rotational stiffness at the slab edge from a mechanical standpoint. At the boundary, it reduces the curvature demand of a given bending moment. This leads to less rotation and deflection near the opening. The applied load, however, does not change, and the global equilibrium must still be satisfied. The decrease in curvature near the boundary thus requires a redistribution of deformation along the slab. This results in a compatibility adjustment of the bending distribution, not a change in the fundamental load path. Therefore, the edge beam serves as a boundary stiffener rather than a new load-carrying mechanism.

3.2 Preservation of Global Load Path

The distributions of the reactions along the supporting walls reveal the load-flow mechanisms. A fundamental change in the global load path from the addition of an edge beam would substantially alter the normalized reaction distribution along the culvert length. However, the numerical results show that the normalized distribution profile remains largely unchanged despite increased reaction magnitudes in the presence of an edge beam. This indicates: 1) The fundamental load-transfer mechanism of the plate is preserved. 2) The edge beam increases the stiffness participation without redirecting the load flow. In other words, the edge beam changes the boundary stiffness, not the plate's action. This distinction is important: a change in magnitude without a change in the distribution shape indicates amplification of participation rather than a shift in the fundamental load-transfer mechanism.

3.3 Conceptual Decay Representation

The variation of the stiffness participation longitudinally can be viewed as a decay function with the following features: i) It peaks near the boundary, ii) It drops off with the normalized distance, and iii) It approaches unity (no amplification) near the mid-length. This behavior is consistent with stiffness-controlled attenuation and suggests the potential to develop a compact decay-based formulation for edge-beam participation. Such a formulation depends on the following parameters: Normalized longitudinal distance, Span, and Relative stiffness contrast between the edge beam and the slab. The development of this formulation provides a mechanically consistent basis for quantifying boundary stiffening effects.

4. RESULTS AND INTERPRETATION

4.1 Load–Deflection Response

Figure 4 and 5 represent the load-deflection responses of the culvert configurations of span=3.08m, 4.26m and 5.48m for 5 selected load positions at distance of 610mm, 914mm, 1422mm, 1829mm and 2743mm from the opening to capture the linear-elastic behavior and further the stiffness extraction. The finite element models are based on linear-elastic material properties and small-deformation assumptions; the response is strictly proportional, and the load-deflection relationship is linear. Therefore, the absolute values of the applied load and the corresponding deflection do not determine stiffness; rather, stiffness is defined as the slope of the linear response,

$$K = \frac{\Delta P}{\Delta \delta}$$

Only a small range of deflection is shown for clarity, and the slope of this response is used to calculate elastic stiffness. Figure 6 shows the load-deflection responses as well as the stable stiffness (K) for both the edge beam case and the no-edge beam cases, specifically for the 3.04m span culvert, for three specific load positions. Rk represents the following ratio:

$$Rk = \frac{K_{\mathrm{EB}}}{K_{\mathrm{NoEB}}}$$

Similar trends, stiffness values, and stiffness ratios were observed and analyzed for all positions and spans.

4.2. Spatial Variation of Stiffness vs Position

Figure 7 shows the variation in stiffness along the culvert length for all the span culverts, both with EB and no-EB cases separately. The slope of the linear load-deflection response at each load position was used to determine the stiffness values. For the No-EB configuration, the stiffness distribution is slightly concave (arch-shaped) along the culvert length. The stiffness is slightly lower near the opening, increases moderately at intermediate locations, and then decreases again towards the midspan. This is the typical behavior of the slab-plate of the box system without local boundary stiffening. Instead, there is no initial region of increased stiffness in the system without additional rotational restraint, but the stiffness increases marginally as the slab's participation becomes more distributed away from the opening, then drops again as the system becomes span-dominated and flexible. In contrast, the EB-culvert configuration clearly shows that stiffness decreases as the distance from the opening increases. The maximum stiffness is found near the opening, where the edge beam provides local boundary stiffening. This amplification gradually decreases towards midspan, approaching the No-EB stiffness values. This clear difference between these stiffness profiles is proof that the edge beam influences the spatial distribution of the culvert's stiffness.

4.3 Reaction Distribution and Load Transfer Mechanism

Figure 7 shows the spatial variation of stiffness for both EB and no-EB configurations, which was further interpreted by analyzing the reaction distributions along the culvert walls at representative load positions of 610 mm, 1420mm, and 1829mm from the opening, as shown in Figures 8, 9, and 10. These are the positions in the near-boundary region, the intermediate transition zone, and the region approaching midspan, respectively. The loading at 0.61 m from the opening indicates a significant amplification of reactions near the boundary, suggesting increased local stiffness and higher load participation around the opening due to the edge beam. On the contrary, the reaction magnitudes in the No-EB case are relatively lower, indicating less boundary restraint. At the intermediate position (1.42 m), the difference between EB and No-EB cases is still visible but reduced in magnitude, indicating a gradual attenuation of the edge-beam influence. The reaction profiles have similar shapes in the EB and NoEB cases, indicating that the primary load-transfer mechanism remains the same. Going away from the inlet (at 1.83 m), the reaction distributions for EB and No-EB configurations become more similar, and the differences in magnitude become small. This convergence indicates that the contribution from the edge beam is negligible at larger distances and the system is mainly governed by the global slab action. Importantly, the overall shape of the reaction distributions appears similar between the EB and No-EB cases for all positions considered. This means that the edge beam does not change the basic load-transfer mechanism but rather increases the reactions in a localized region near the boundary. The observations provide direct mechanical evidence that the edge beam acts as a boundary-stiffening element, with a spatially localized effect that decays progressively with distance along the culvert.

5. RELATIVE STIFFNESS PARTICIPATION OF THE EDGE BEAM

Figure 11 shows the global vs relative stiffness behavior along the length of the slab for the culvert configuration with edge beam. To isolate the incremental stiffness contribution of the edge beam independent of global stiffness magnitude, a relative stiffness ratio was defined as:

$$Rk = \frac{K_{\text{EB}}}{K_{\text{NoEB}}}$$

The relative stiffness represents the isolated effect of the edge beam, propagating in the slab. A representative exponential function was fitted for relative stiffness Rk data points to best represent the exponential decay effect. Figure 12 presents the variation of Rk for all considered spans. For each span, the relative stiffness peaks near the opening region and progressively decreases toward unity as distance increases. The consistently decreasing trend across spans confirms that the edge beam introduces a localized, boundary-controlled stiffness enhancement that decays spatially along the culvert length, irrespective of span. In addition, a representative exponential function was fitted to the relative stiffness curve to further inform about the nature of the edge beam stiffness decay.

6. GENERALIZED MODEL FOR RELATIVE STIFFNESS PARTICIPATION

6.1 Functional Form Selection

The relative stiffness distributions presented in the previous section exhibit a consistent spatial pattern across spans. The stiffness ratio remains close to unity near the mid-length and increases to a local maximum at small distances from the opening. This behavior indicates that the edge beam introduces localized stiffness amplification that develops over a short influence region and decays progressively along the culvert length. The resulting generalized formulation is expressed as:

$$R(\eta, S) = 1 + A \left(\frac{S}{S_0}\right)^m \eta e^{-B\eta} \tag{1}$$

$$\eta = \frac{z - z_0}{L - z_0} \tag{2}$$

To account for the observed variation in amplification magnitude across spans, a span-scaling term $\left(\frac{S}{S_0}\right)^m$ was introduced, where S is the culvert span, and S_0 is the reference span used for normalization. Here, A, m, and B are regression parameters to be determined. It is to be noted that the study was not undertaken to generalize across all configurations and load positions but to establish a representative mathematical expression that could reveal stiffness participation. Therefore, the model was calibrated for

$$z \geq 0.610 \text{ m}$$

6.2 Regression Procedure

The regression was performed using stiffness ratios obtained from linear-elastic finite-element analyses across multiple spans and load positions. For each configuration, the effective stiffness was extracted from the slope of the initial linear portion of the load–deflection response using least-squares fitting. Because all models employed purely linear elastic material properties, the extracted slope corresponds to the system's constant global stiffness at the selected load location. For each span normalized position =z/L, the relative stiffness ratio was computed as:

$$R(\eta, S) = \frac{k_{\text{with}}(\eta, S)}{k_{\text{no}}(\eta, S)} \tag{3}$$

Only valid data pairs with finite and positive stiffness values were retained. To reduce numerical sensitivity due to floating-point precision, stiffness values were rounded to a fixed decimal resolution before ratio computation, without affecting the underlying elastic trend. The regression was conducted simultaneously over all spans using nonlinear least-squares minimization. The objective function minimized the sum of squared errors between the measured ratios, R_i, and the model predictions.

$$\min_{A,m,B} \sum_i \left[R(\eta_i, S_i) - R_i\right]^2 \tag{4}$$

To ensure physically meaningful parameters, logarithmic transformations were applied to enforce positivity of the amplification parameter A and decay parameter B during optimization. The parameters were estimated using an unconstrained nonlinear optimization algorithm (Nelder–Mead method). Model performance was evaluated using the coefficient of determination, R^2, computed with respect to the relative stiffness ratio R. Fitting was performed directly on R, rather than on the reduced quantity $R - 1$, which improves numerical stability in regions where the edge-beam influence becomes small.

6.3 Interpretation of Model Parameters

The proposed formulation

$$R(\eta, S) = 1 + A \left(\frac{S}{S_0}\right)^m \eta e^{-B\eta} \tag{5}$$

The proposed expression provides a compact representation of the edge beam's spatial stiffness participation. The model was calibrated using discrete load positions beginning at $z_0 = 0.610$ m from the culvert opening. Therefore, the normalized load position was defined as

$$\eta = \frac{z - z_0}{L - z_0} \tag{6}$$

where z is the load position, $z_0 = 0.610$ m is the first calibrated load position, and L is the culvert length. For the present study, culvert length is $L = 7.315$ m,

$$\eta = \frac{z - 0.610}{7.315 - 0.610} \tag{7}$$

Values outside the calibrated range correspond to extrapolation and are not used for interpretation.

The constant term "1" represents the baseline No-EB condition. As the edge-beam influence diminishes with distance, the relative stiffness approaches unity, satisfying the physical condition that $R \to 1$ when the edge-beam contribution becomes negligible.

The parameter A governs the magnitude of stiffness amplification due to the edge beam, while B

controls the spatial decay rate of this influence along the culvert length. Larger values of B indicate faster attenuation of the edge-beam effect. The exponent m controls how the stiffness amplification scales with span length through the term $(S/S_0)^m$.

In this study, the edge-beam geometry, slab thickness, and material properties are maintained constant, while span length is varied. Therefore, A and B are treated as constants for the selected structural configuration, and the span effect is incorporated through $(S/S_0)^m$.

Collectively, the parameters describe: (i) the magnitude of stiffness amplification, (ii) its dependence on span length, and (iii) the spatial attenuation of edge-beam participation.

6.4. Model Performance and Validation

The predictive capability of the proposed relative stiffness formulation was evaluated by comparing the model predictions with the finite element results across all training spans and load positions. Figure 13 presents the fitted curves together with the extracted relative stiffness ratios for the 3.048 m, 4.267 m, and 5.486 m spans. The smooth curves represent the generalized expression,

$$R(\eta, S) = 1 + A\left(\frac{S}{S_0}\right)^m \eta e^{-B\eta} \tag{8}$$

while the markers denote stiffness ratios computed directly from the finite element simulations. The normalized load position was defined as

$$\eta = \frac{z - z_0}{L - z_0} \tag{9}$$

where z is the load position measured from the culvert opening, $z_0 = 0.610$ m is the first evaluated load position, L is the culvert length, S is the culvert span, and S_0 is the reference span.

The fitted model shows strong agreement with the numerical results, with a coefficient of determination of $R^2 = 0.97$. This indicates that the proposed formulation captures the dominant spatial trend governing the edge beam's contribution to stiffness. The model reproduces key behavioral features observed in the data: (i) the presence of a peak amplification within a finite influence region, and (ii) the progressive decay toward unity as the load position approaches the mid-length region.

Although minor separation between span-specific curves persists across the domain, including toward mid-length, this variation is small relative to the overall amplification magnitude. Such differences reflect variations in global flexibility and slab–wall interaction associated with span length that are not fully removed by normalization. Importantly, the consistent convergence toward $R \approx 1$ with increasing normalized distance confirms that edge-beam participation is a localized, boundary-controlled effect whose relative influence diminishes along the culvert length.

To further assess generality, independent span–position combinations not included in the regression dataset were evaluated for validation cases, as shown in Figure 14. These included a 3.658 m span at $z = 0.762$ m and a 4.877 m span at $z = 2.286$ m. For each configuration, stiffness was extracted using the same linear-slope procedure, and the predicted ratio was computed using the calibrated model parameters. The validation results show close agreement with the finite element data, with percentage errors remaining within acceptable limits.

Overall, the regression results demonstrate that a single span-sensitive exponential formulation can effectively describe the spatial amplification and attenuation of relative stiffness across multiple geometries. The high coefficient of determination and the agreement observed in the validation cases support the use of the proposed formulation as a compact representation of edge-beam stiffness participation within the calibrated service-level response range.

6.5. EDGE BEAM CONTRIBUTION INDEX

To further illustrate the contribution of the edge beam, an Edge Beam Contribution Index (EBCI) is defined as "EBCI"=R-1, and is presented as a function of position in Figure 15. This representation directly quantifies the additional stiffness contribution from the edge beam relative to the baseline (No-EB) condition. The EBCI profiles show a clear peak near the opening, followed by a gradual reduction toward zero with increasing distance, consistent with the observed decay behavior. As the load position approaches midspan, EBCI values converge toward zero, indicating negligible edge-beam influence. This formulation provides a more intuitive interpretation of stiffness amplification by isolating the edge beam's net contribution to the total stiffness response.

7. ENGINEERING APPLICATION

The proposed framework offers a rational basis for interpreting stiffness-driven load distribution in box culvert systems by explicitly quantifying the spatial variation in relative stiffness participation attributable to the edge beam. Identification of a consistent decay-type behavior, characterized by a limited set of physically interpretable parameters, enables a structured understanding of how boundary stiffening influences slab response along the culvert length. This formulation allows one to represent the non-uniform distribution of stiffness participation in simplified analyses or assessments, where conventional models assume a uniform distribution. The present study aids in the better interpretation of structural response and informs future assessment-oriented methodologies.

8. SUMMARY

The study investigated the spatial variation of the effective stiffness of reinforced-concrete box culverts and quantified the edge-beam effect with linear-elastic finite-element analysis of typical-span culverts. Results show that culvert systems do not have uniform stiffness, contrary to the assumption typically made in design and analysis. As a result of plate action and boundary effects, the stiffness varies along the length of the culvert. The presence of an edge beam causes a localized amplification of stiffness near the opening, while the overall load-transfer mechanism remains unchanged. The reaction distributions indicate that the edge beam is primarily a boundary-stiffening element, increasing reaction magnitudes without affecting the global load path. To separate the contribution of the edge beam, a relative stiffness parameter was introduced. The resulting trends show a consistent pattern of stiffness amplification followed by spatial decay as distance increases. On this basis, a span-sensitive formulation is developed to capture the contribution of edge-beam stiffness as a function of position and span length. The proposed model is in good agreement with finite element results, with a coefficient of determination $R^2 = 0.97$.

The proposed formulation provides a physically interpretable framework for quantifying edge-beam participation and helps improve understanding of the stiffness-controlled behavior of short-span bridge systems.

REFERENCES

Abdel-Karim, A. M., Tadros, M. K., and Benak, J. V. (1993). "Structural response of full-scale concrete box culvert." *Journal of Structural Engineering*, 119(11), 3238–3254.

Bentz, E. C., Yee, R., and Collins, M. P. (2007). "Investigating the shear strength of concrete box culverts." *Transportation Research Board Annual Meeting*.

Fuchs, S. J. (1954). "Plates with boundary conditions of elastic support." *Transactions of the American Society of Civil Engineers*, 119(1), 7–46.

Hu, D. and Adams, G. G. (2017). "A boundary condition correction for the clamped constraint of elastic plate/beam theory." *International Journal of Solids and Structures*, 49(19–20), 2747–2757.

Liu, Y., Schindler, A. K., and Davidson, J. S. (2018). "Finite-element modeling and analysis of early-age cracking risk of cast-in-place concrete culverts." *Transportation Research Record*, 2672(27), 24–36.

Mabsout, M., Tarhini, K., Jabakhanji, R., and Awad, E. (2004). "Wheel load distribution in simply supported concrete slab bridges." *Journal of Bridge Engineering*, 9(2), 147–155.

Moradi, M., Valipour, H., and Foster, S. (2015). "Reserve of strength in inverted u-shaped rc culverts: Effect of backfill on ultimate load capacity and fatigue life." *Journal of Bridge Engineering*.

Orton, S. L., Loehr, J. E., Boeckmann, A., and Havens, G. (2015). “Live-load effect in reinforced concrete box culverts under soil fill.” *Journal of Bridge Engineering*, 20(11).

Ulger, T., Okeil, A. M., and Elshoura, A. (2020). “Load testing and rating of cast-in-place concrete box culverts.” *Journal of Performance of Constructed Facilities*.

Woo, S. K., Jo, J. H., and Kwon, Y. G. (2010). “Failure behavior characteristics of box culvert using 3-axes loading system.” *Fracture Mechanics of Concrete and Concrete Structures: High Performance, Fiber Reinforced Concrete, Special Loadings and Structural Applications*, Korea Concrete Institute.

List of Figures

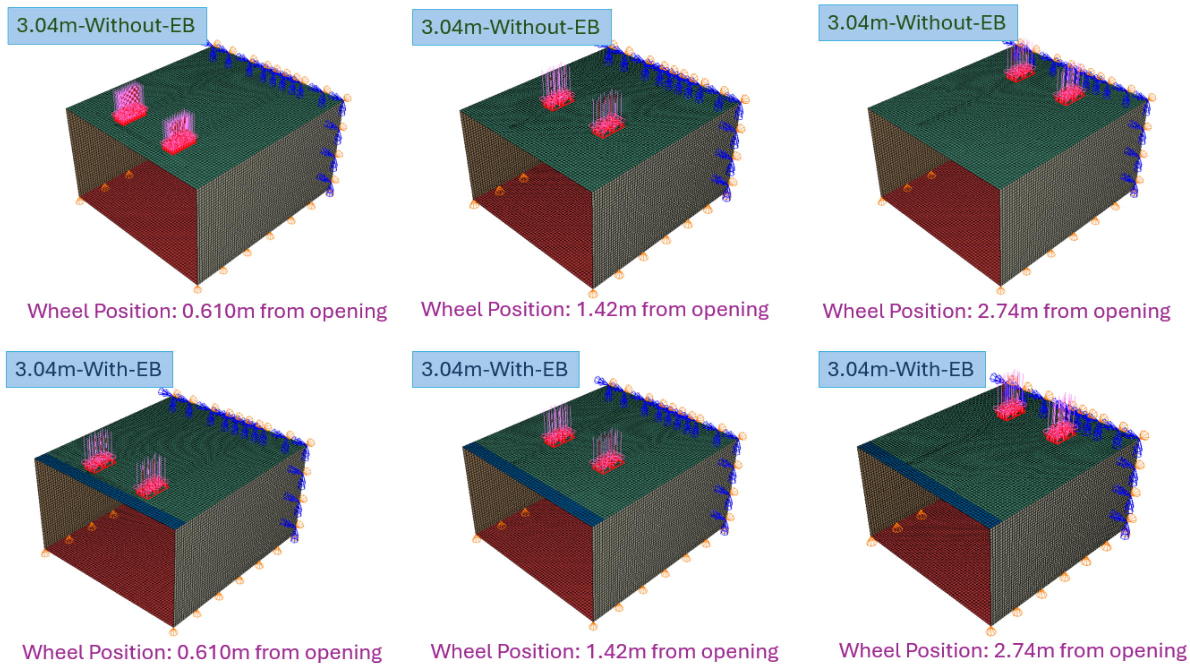

Fig. 1. Representative finite element models showing loading configurations at selected positions

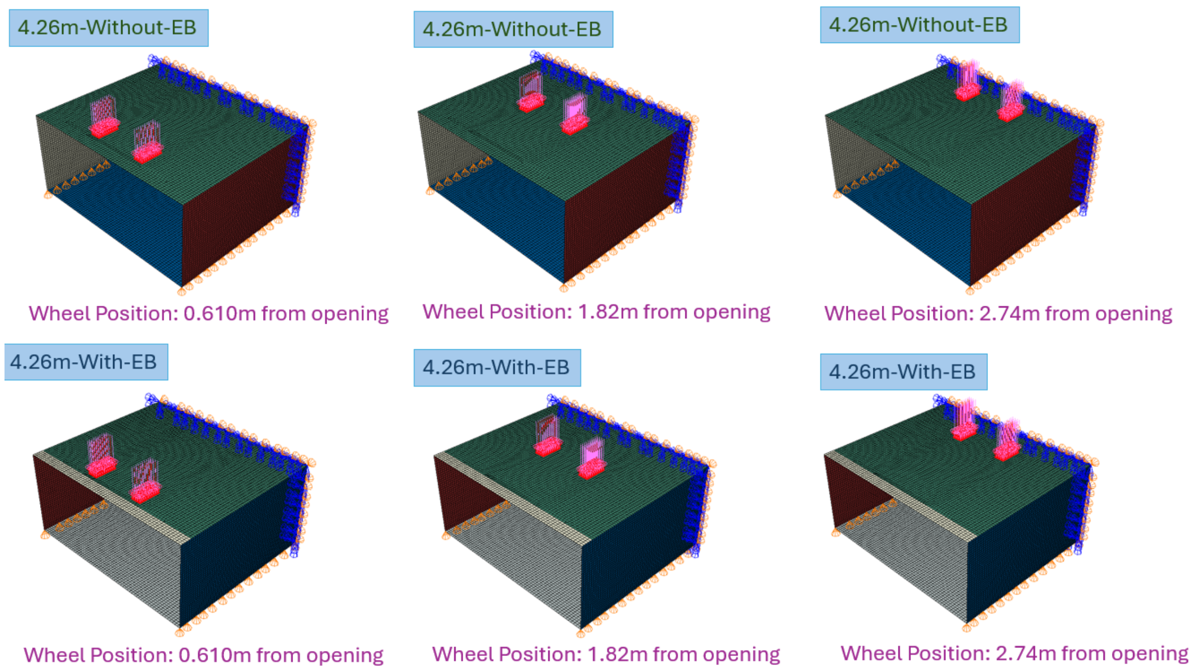

Fig. 2. Representative finite element models showing loading configurations at selected positions

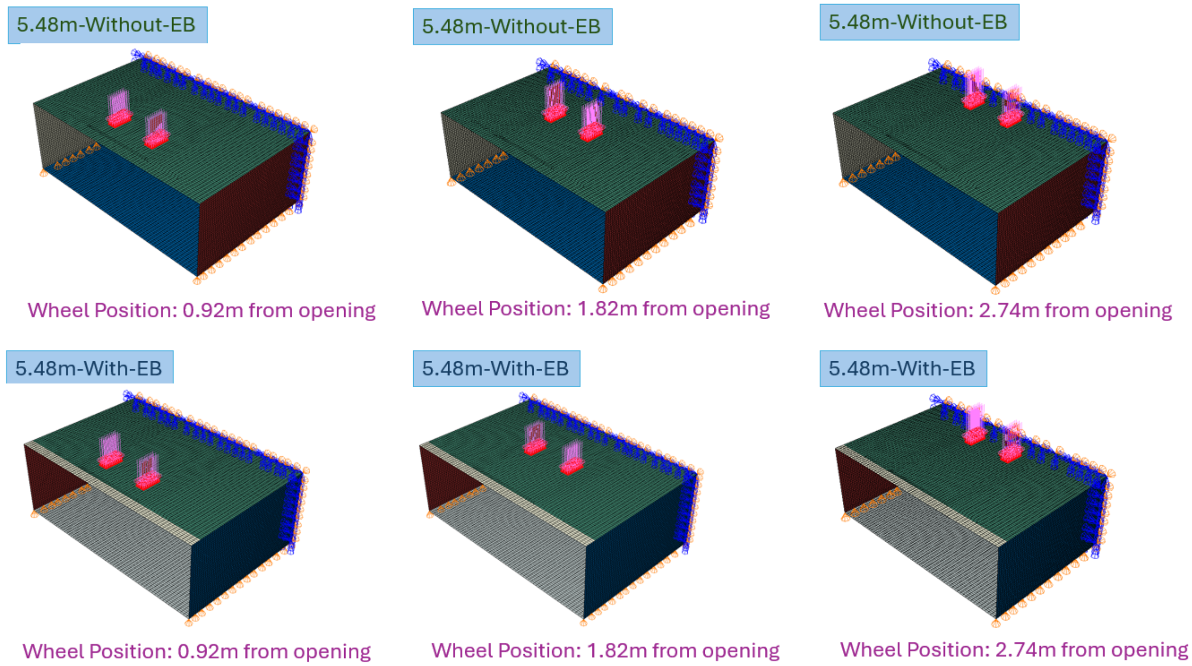

Fig. 3. Representative finite element models showing loading configurations at selected positions

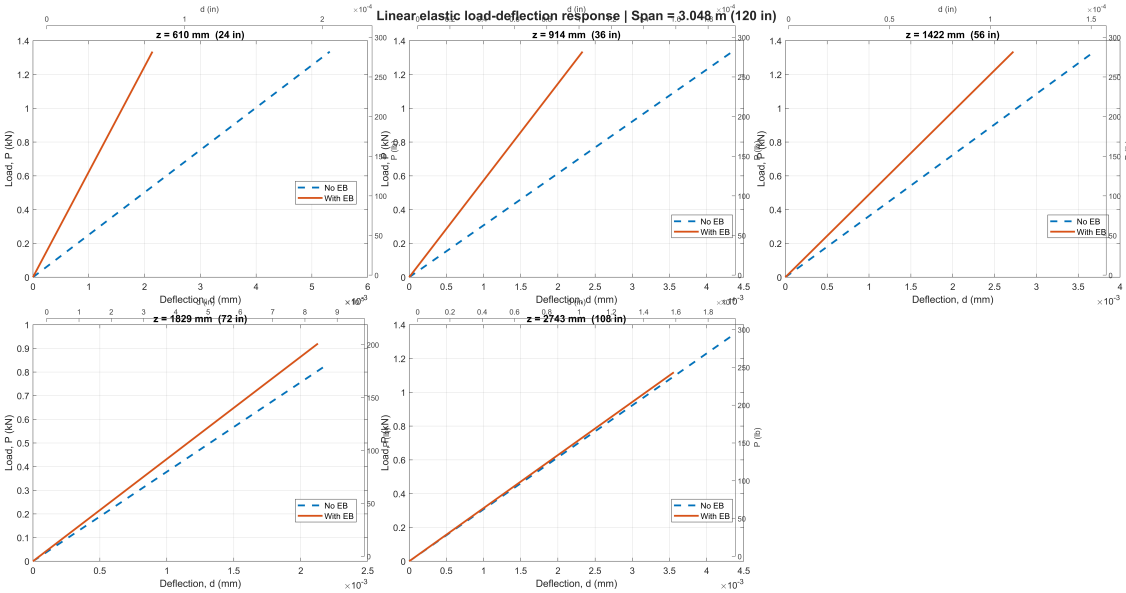

(a) Span = 3.04 m

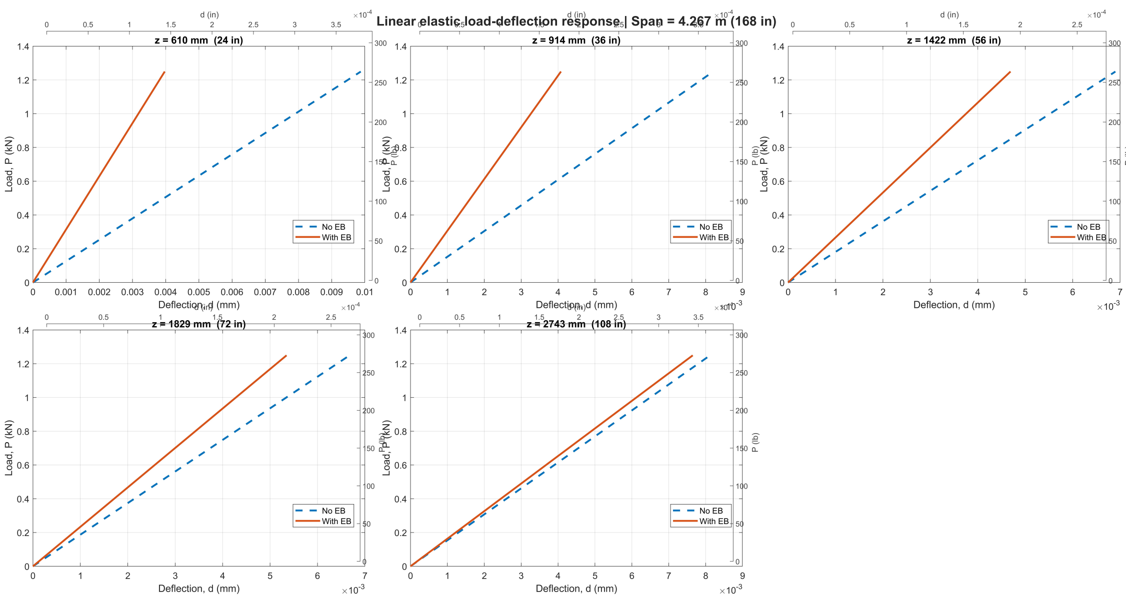

(b) Span = 4.26 m

Fig. 4. Load–deflection responses for culvert models with spans of 3.04 m and 4.26 m.

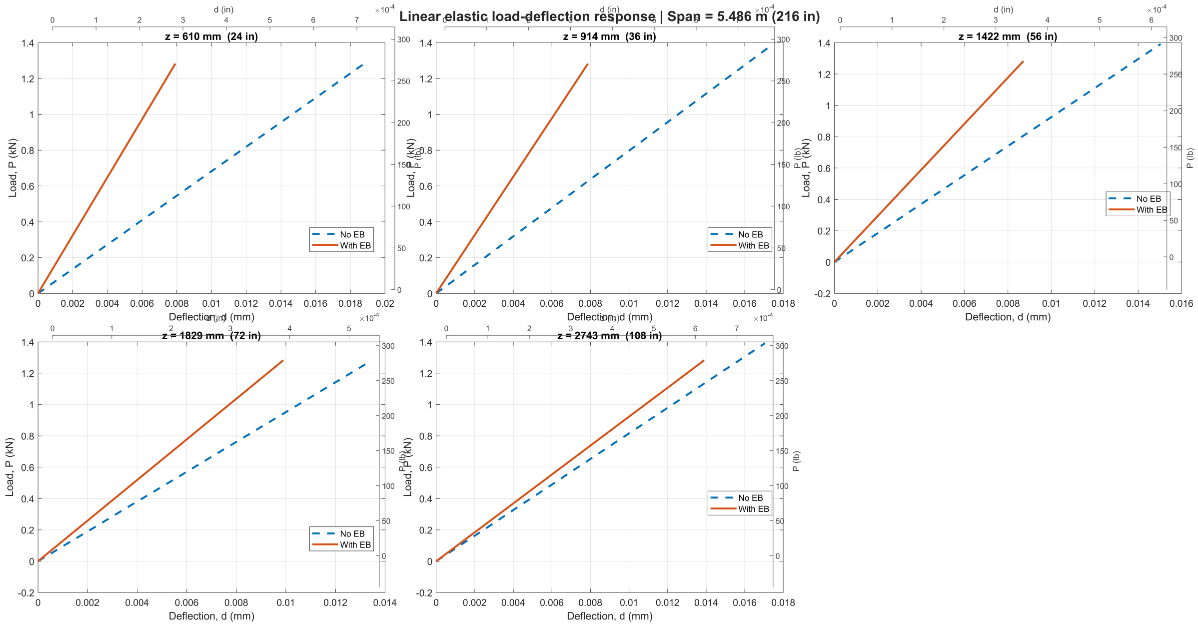

(c) Span = 5.48 m

Fig. 5. Load–deflection response for the culvert model with span of 5.48 m.

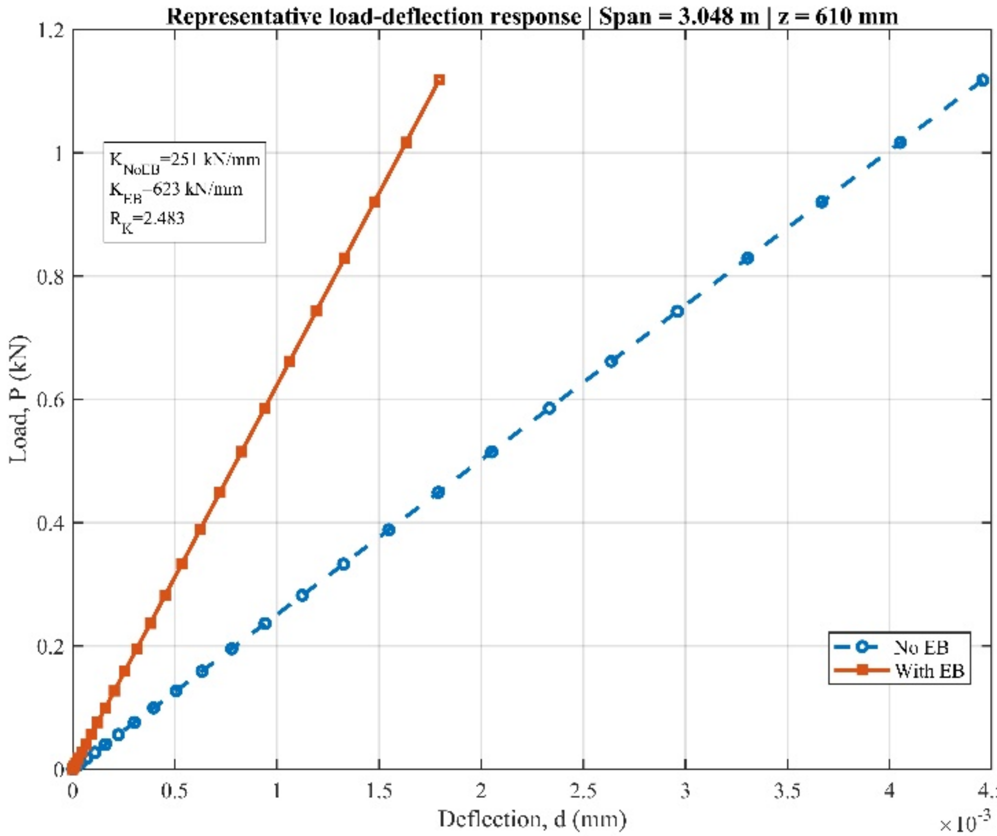
Representative load-deflection response | Span = 3.048 m | z = 610 mm
K_NoEB=251 kN/mm
K_EB=623 kN/mm
R_K=2.483
Load, P (kN)
Deflection, d (mm)
×10^-3
No EB
With EB

(a) 0.61 m

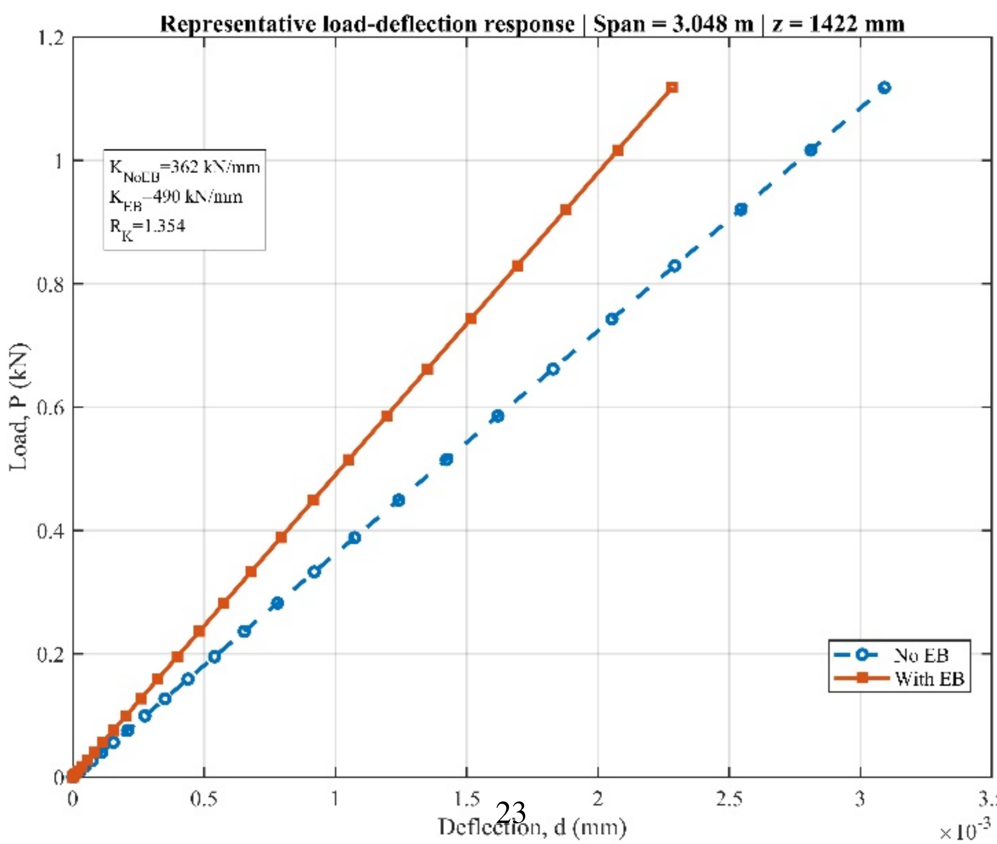
Representative load-deflection response | Span = 3.048 m | z = 1422 mm
K_NoEB=362 kN/mm
K_EB=490 kN/mm
R_K=1.354
Load, P (kN)
Deflection, d (mm)
×10^-3
No EB
With EB

(b) 1.42 m

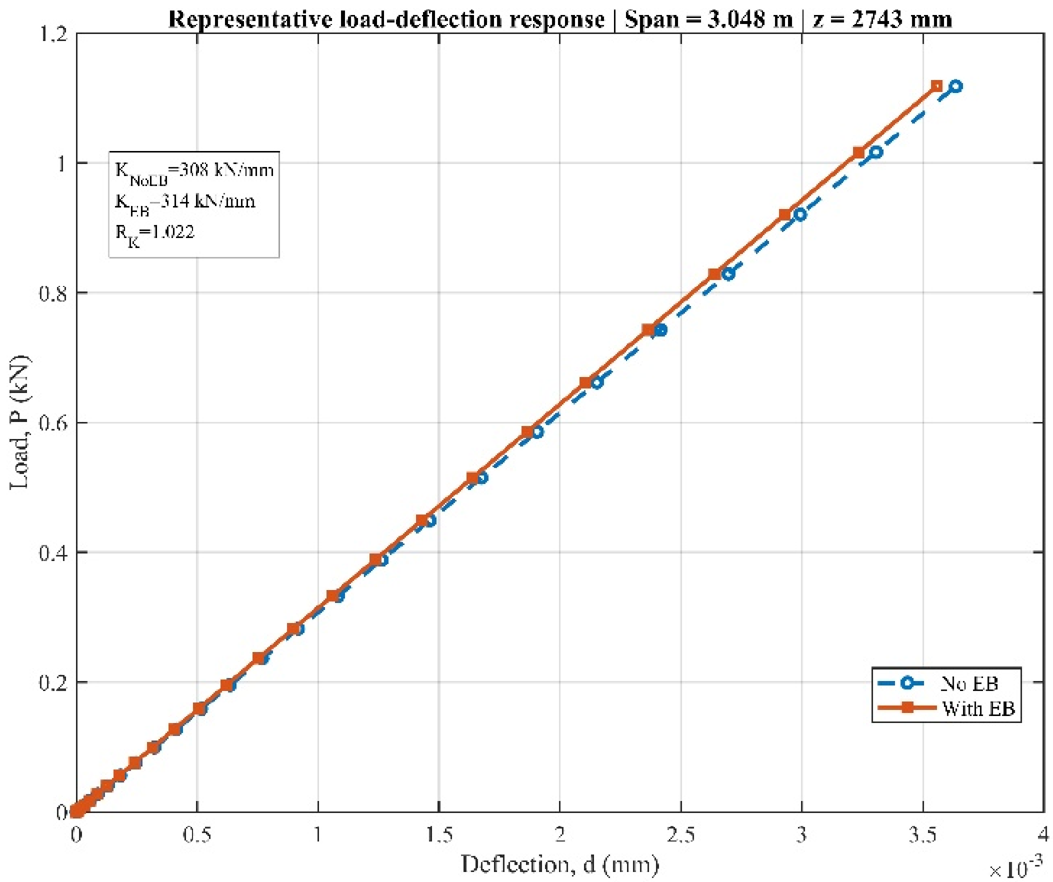

(c) 2.74 m

Fig. 6. Load–deflection responses for the 3.04 m span culvert at selected load positions from the culvert opening: (a) 0.61 m (b) 1.42 m (c) 2.74 m.

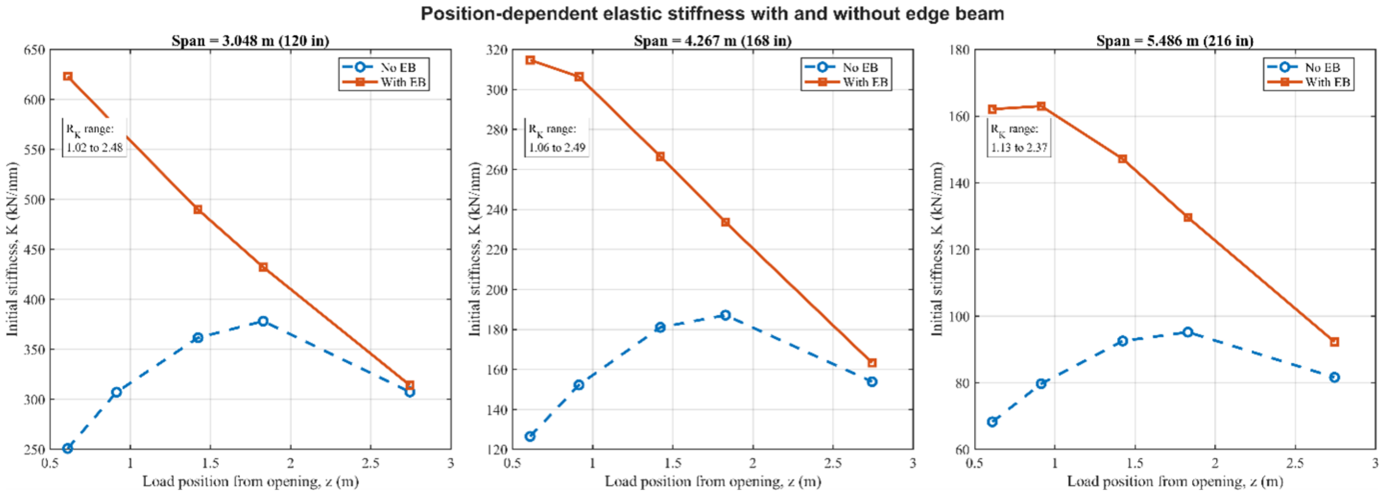

Fig. 7. Position-dependent stiffness response of the culvert models with and without the edge beam.

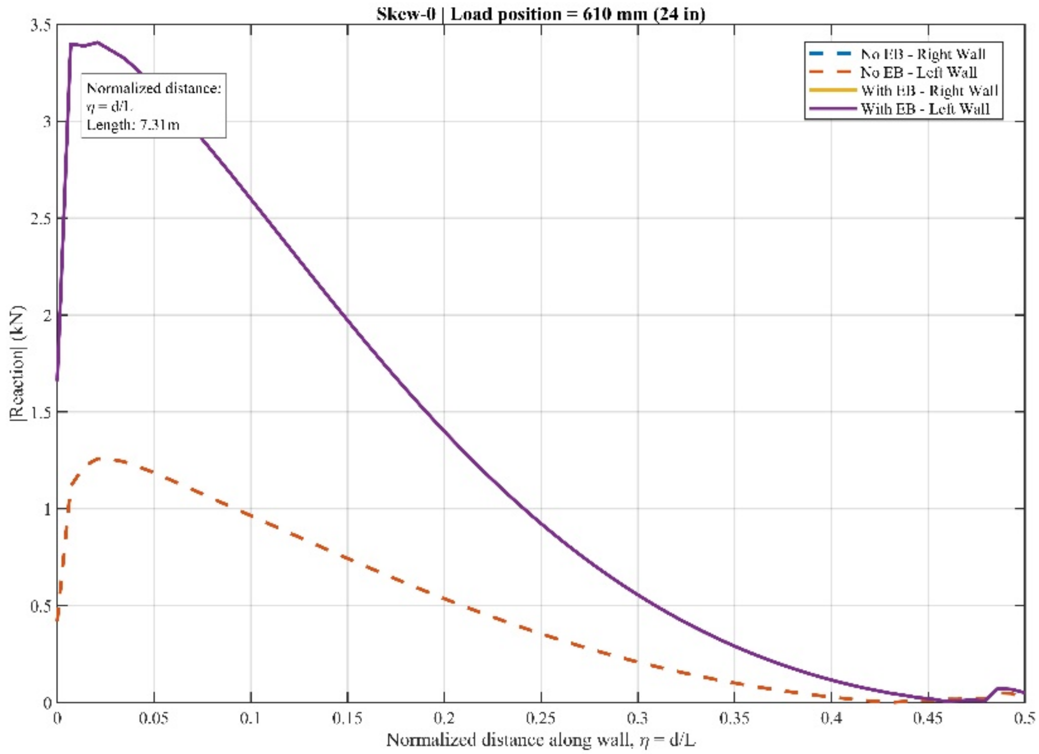

Fig. 8. Reaction vs Normalized Distance for load position = 610 mm

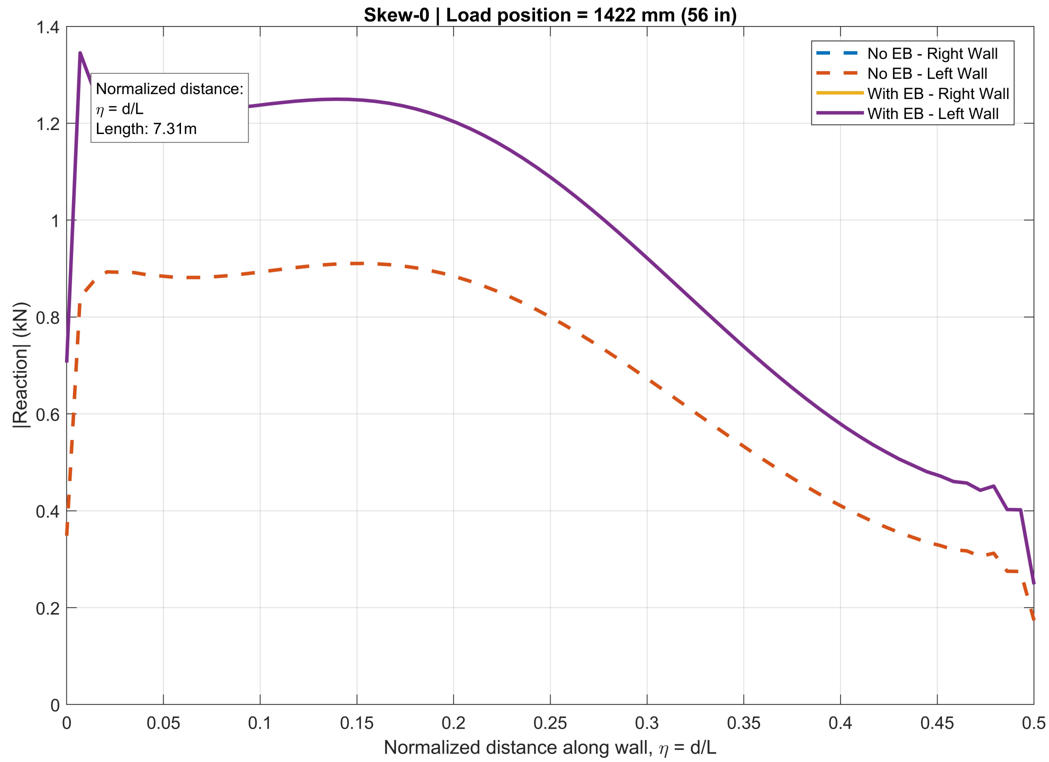

Fig. 9. Reaction vs Normalized Distance for load position = 1422 mm

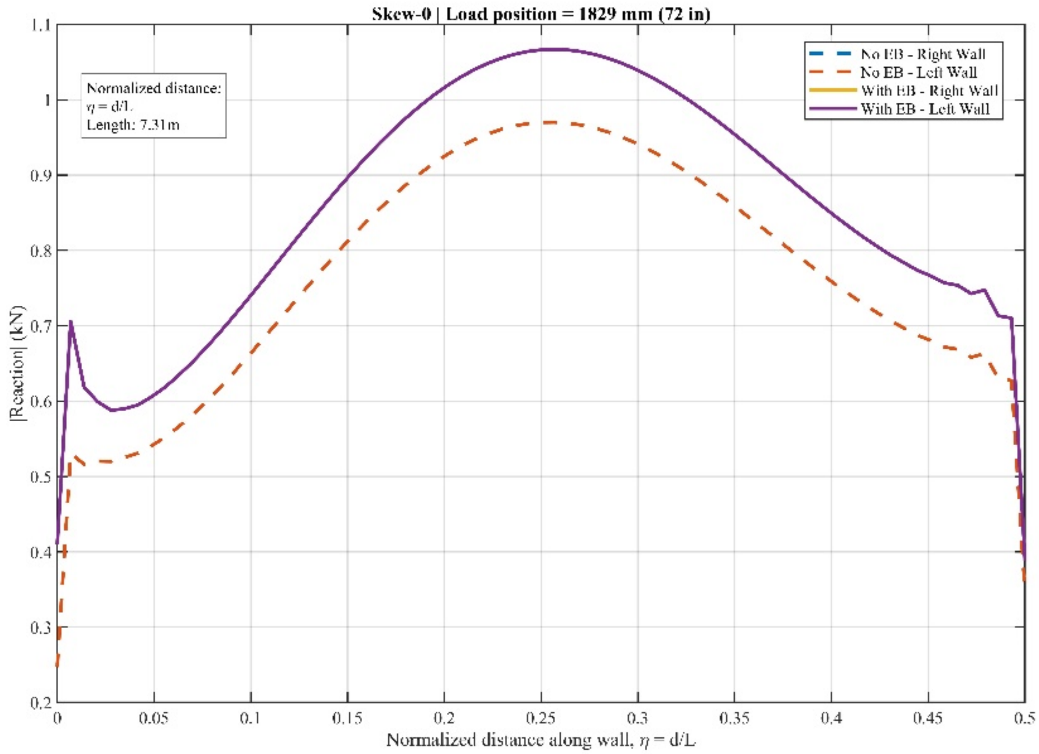

Fig. 10. Reaction vs Normalized Distance for load position = 1829 mm

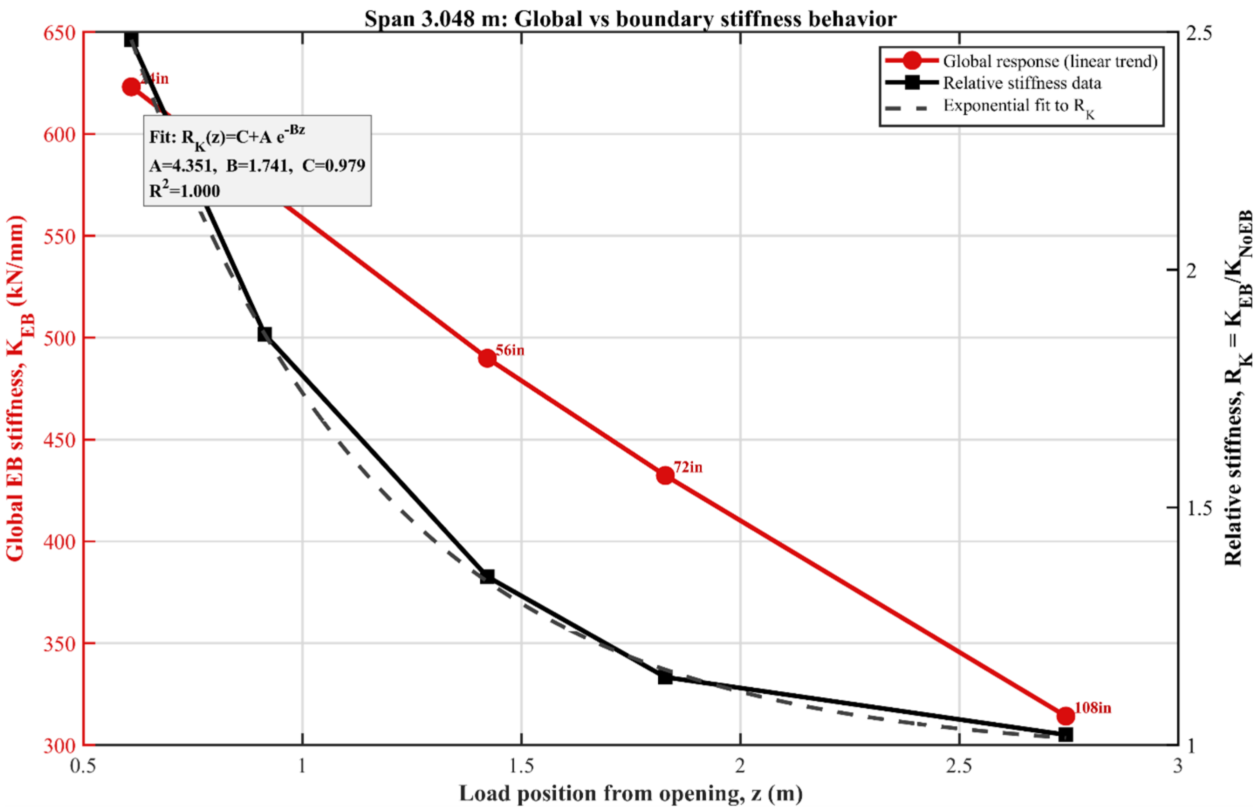

Fig. 11. Global vs Relative Stiffness behavior

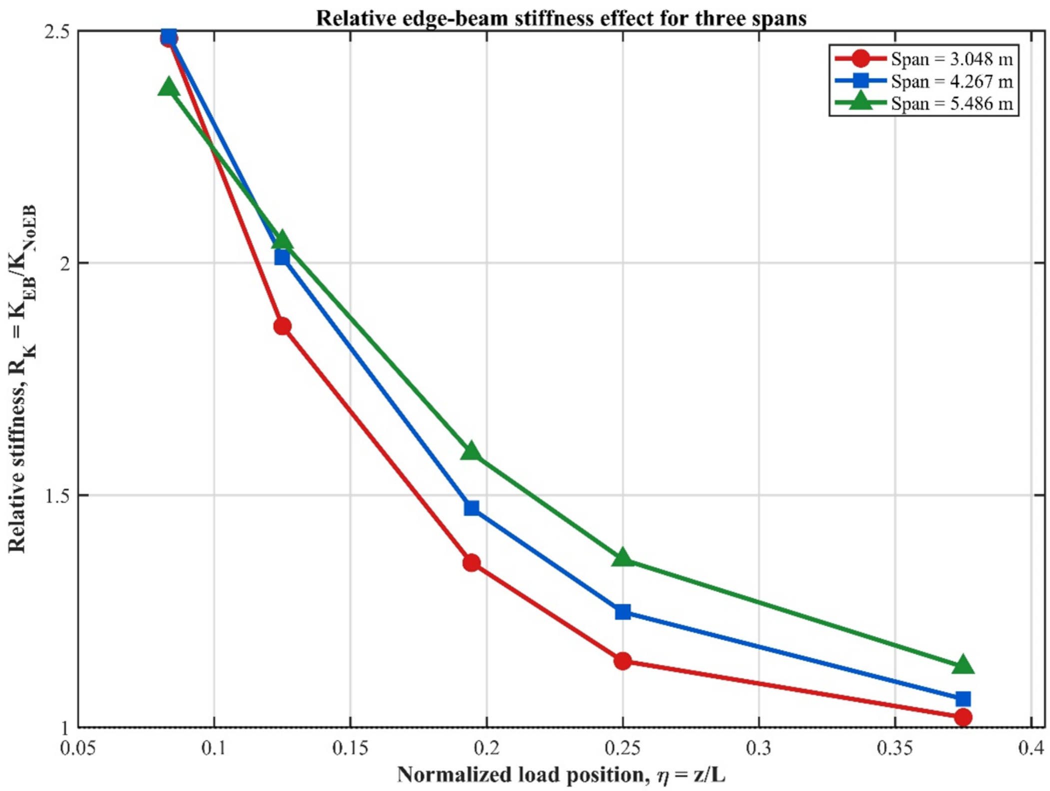

Fig. 12. Relative Edge Beam Stiffness for all spans

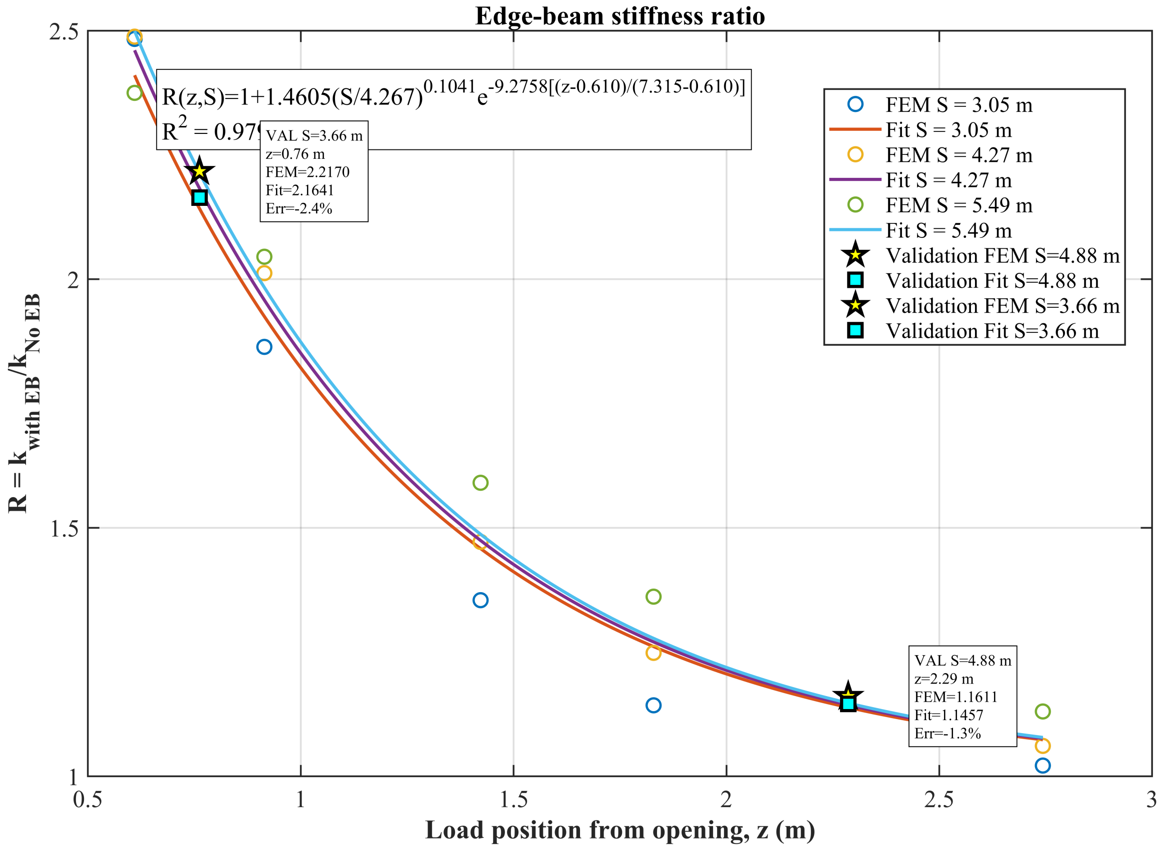

Fig. 13. Edge Beam Stiffness Equation

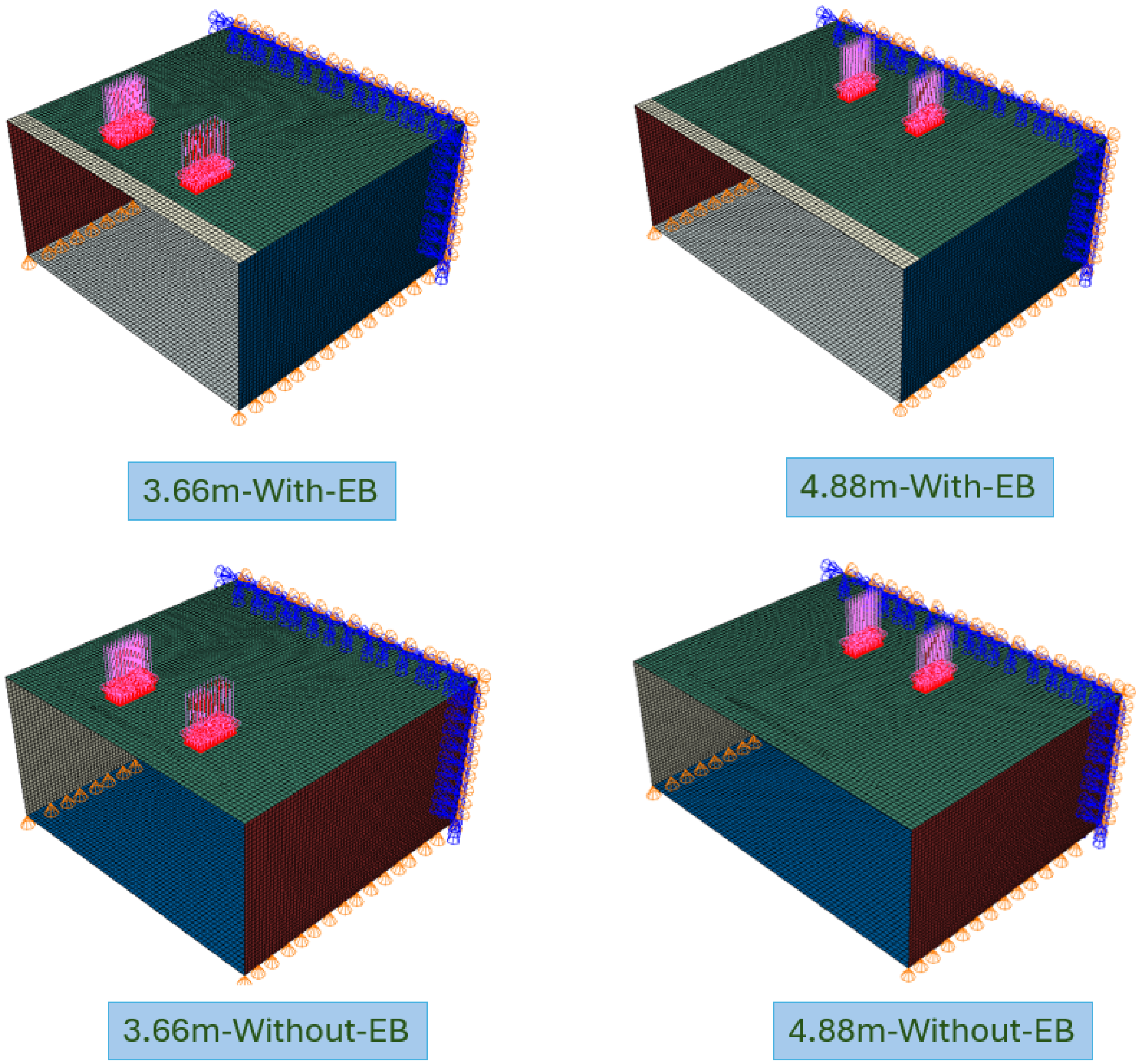

Fig. 14. Finite Element Models for Validation Purposes

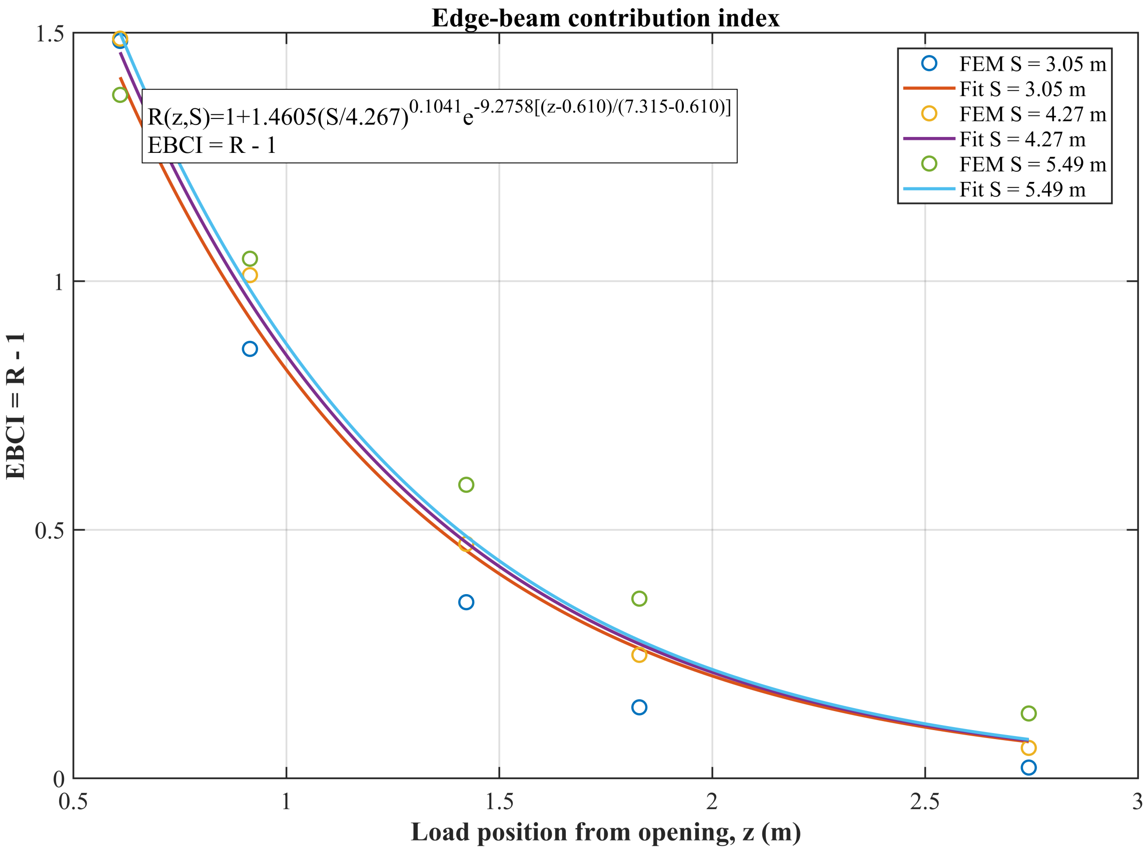

Fig. 15. Edge Beam Stiffness Contribution